Title
Boundary layer control of rotating convection systems

Journal
Nature, 457(7227)

ISSN
0028-0836

Authors
King, Eric M
Stellmach, Stephan
Noir, Jerome
et al.

Publication Date
2009

DOI
10.1038/nature07647

Peer reviewed

LETTERS

Boundary layer control of rotating convection systems

Eric M. King[1], Stephan Stellmach[2]†, Jerome Noir[1], Ulrich Hansen[2] & Jonathan M. Aurnou[1]

Turbulent rotating convection controls many observed features of stars and planets, such as magnetic fields, atmospheric jets and emitted heat flux patterns[1–6]. It has long been argued that the influence of rotation on turbulent convection dynamics is governed by the ratio of the relevant global-scale forces: the Coriolis force and the buoyancy force[7–12]. Here, however, we present results from laboratory and numerical experiments which exhibit transitions between rotationally dominated and non-rotating behaviour that are not determined by this global force balance. Instead, the transition is controlled by the relative thicknesses of the thermal (non-rotating) and Ekman (rotating) boundary layers. We formulate a predictive description of the transition between the two regimes on the basis of the competition between these two boundary layers. This transition scaling theory unifies the disparate results of an extensive array of previous experiments[8–15], and is broadly applicable to natural convection systems.

Rapidly rotating convection is typically organized by the Coriolis force into tall, thin, coherent convection columns that are aligned with the rotation axis (Fig. 1a). This organizing effect is thought, for example, to be responsible for the strength and structure of magnetic fields generated by convection in planetary interiors[16]. As thermal forcing is increased, the relative influence of rotation weakens, and three-dimensional, turbulent convection can occur (Fig. 1b). It is commonly assumed that rotational effects will dominate convection dynamics when the ratio of the global buoyancy force to the Coriolis forces is less than unity[7–12]. Here we argue, by means of a coupled set of laboratory and numerical experiments, that the boundary layer dynamics, not the global force balance, control the style of convection.

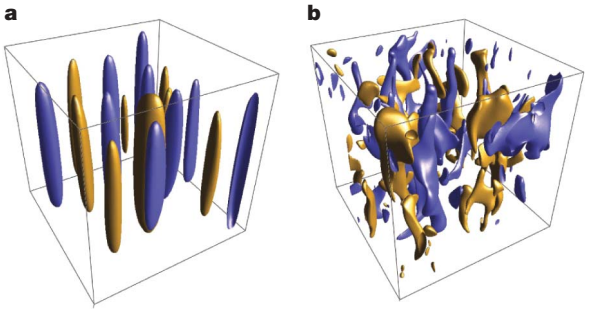

Figure 1 | Iso-surfaces of vertical velocity, from numerical experiments. **a**, $E = 10^{-4}$, $\mathrm{Ra} = 5 \times 10^6$, $\mathrm{Pr} = 7$. Here we see large-scale, coherent, axially aligned velocity structures typical of rotationally dominated convection. $\mathrm{Ro_c} = 0.08$, $\mathrm{Ra/Ra_t} = 0.36$. **b**, $E = 10^{-4}$, $\mathrm{Ra} = 2.1 \times 10^8$, $\mathrm{Pr} = 7$. Here we see predominantly three-dimensional convective structures typical of non-rotating convection, despite a ratio of global buoyancy to Coriolis force of $\mathrm{Ro_c} = 0.5$. However, the boundary-layer-transition hypothesis predicts this breakdown of rotational control, as $\mathrm{Ra/Ra_t} = 14$.

Many previous studies of heat transfer exist for rotating convection systems[8–10,12–15]. However, no unified description of rotating convective heat transfer exists. Often, such studies seek scaling laws for heat transfer efficiency as a function of thermal driving, $\mathrm{Nu} \propto \mathrm{Ra}^{\alpha}$. The Nusselt number, Nu, characterizes the efficiency of convective heat transfer, and is given by the ratio of the total heat transfer to the conductive heat transfer. Thus, $\mathrm{Nu} = 1$ for purely conductive heat transfer, and higher values of Nu correspond to more efficient convective heat transfer. The strength of buoyancy forcing is characterized by the ratio of buoyancy to diffusion, quantified by the Rayleigh number, Ra. In thermal convection, $\mathrm{Ra} = \alpha_T g \Delta T D^3/\nu\kappa$, where α_T is the fluid's thermal expansion coefficient, g is the acceleration due to gravity, ΔT is the temperature drop across the fluid layer, D is the length scale of the system, ν is the fluid's viscous diffusivity and κ is the fluid's thermal diffusivity. Many non-rotating convection studies yield a scaling exponent of $\alpha \approx 2/7$ (refs 10, 17, 18). Some rotating convection studies still find the $\alpha \approx 2/7$ scaling[8–10], whereas comparable studies have found a markedly different, $\alpha \approx 6/5$, scaling[12–14]. Extrapolating these two empirical scaling laws to astrophysical or geophysical parameters yields predictions that disagree by many orders of magnitude.

In this Letter, we show that this apparent discrepancy can be explained in terms of boundary layer dynamics. A convecting fluid volume consists of two distinct dynamical regions: the interior (or bulk) fluid, and the boundary layers[1,19]. Typically, most of the convecting volume is contained in the bulk, and the boundary layers are thin regions where the interior fluid meets the bounding surfaces and diffusion is important. In turbulent, non-rotating convection, diffusive effects are negligible in the bulk of the fluid. Ideally, strongly turbulent motions result in a well-mixed, isothermal interior, corresponding to an effective thermal short cut across the fluid layer[1]. The only remaining limitation to heat transfer, then, is in the quasi-static thermal boundary layers. In this system, it can be shown that $\mathrm{Nu} \propto D/\delta_\kappa$, where δ_κ is the thermal boundary layer thickness[1], such that the thermal boundary layer becomes thinner as the vigour of convection is increased (see Supplementary Information, section 2). In rotating fluid dynamics, the strength of rotation is characterized by the ratio of the viscous force to the Coriolis force, namely the Ekman number, $E = \nu/2\Omega D^2$, where Ω is the angular rate of rotation. In rapidly rotating systems, the important boundary layer is the Ekman layer, which promotes communication between the rotating container and the bulk fluid, permitting an interior flow that is controlled by rotation[9,19]. The Ekman boundary layer has thickness $\delta_E \propto E^{1/2}D$, such that the Ekman layer becomes thinner as the system's rotation rate increases.

Following refs 20–22, we hypothesize that the effects of rotation dominate convection dynamics when the Ekman layer is thinner than the thermal boundary layer, that is, when $\delta_E < \delta_\kappa$. By contrast, when

[1]Department of Earth and Space Sciences, University of California, Los Angeles, California 90095-1567, USA. [2]Institut für Geophysik, WWU Münster, AG Geodynamik Corrensstrasse 24, Münster 48149, Germany. †Present address: Department of Applied Mathematics and Statistics, and Institute of Geophysics and Planetary Physics, University of California, Santa Cruz, California 95064, USA.

the thermal boundary layer is thinner than the Ekman layer, $\delta_\kappa < \delta_E$, the uppermost part of the Ekman layer is mixed with the bulk. This mixing truncates the influence of the Ekman layer, and therefore rotation, on the interior fluid dynamics[20,22]. The transition between rotationally controlled and non-rotating convection dynamics therefore occurs when $\delta_\kappa \approx \delta_E$. We solve for a transitional Nusselt number scaling by equating δ_κ and δ_E, yielding $Nu_t \propto E^{-1/2}$. Thus, our hypothesis leads us to predict that convection will be dominated by the influence of rotation when $Nu < Nu_t$. Conversely, we expect non-rotating convection dynamics for $Nu > Nu_t$.

Rotating convection experiments allow us to vary the thickness of the thermal boundary layer by varying the heating rate, and that of the Ekman boundary layer by varying the rotation rate. To test our hypothesis, we carry out laboratory and numerical experiments spanning $2 \times 10^3 < Ra < 6 \times 10^9$ and $10^{-6} \leq E \leq \infty$ (see Supplementary Information, section 1). Heat transfer behaviour is shown in Fig. 2. Non-rotating ($E = \infty$) heat transfer data agree with the previously obtained $Nu \propto Ra^{2/7}$ scaling law[10,17,18]. Several different fluids are used, as characterized by the Prandtl number, $Pr = \nu/\kappa$. Fluids with different Prandtl numbers yield slightly different non-rotating scaling prefactors[23–25], but we do not consider this relatively weak effect here. When rotation is included, the onset of convection is delayed by the stabilizing effect of the Coriolis force[26]. Once convection begins, heat transfer exhibits a much steeper scaling, in agreement with the previously reported $Nu \propto Ra^{6/5}$ relationship[12–14]. More specifically, heat transfer is adequately described by $Nu = (Ra/Ra_c)^{6/5}$ in this convective regime, where $Ra_c = 6E^{-4/3}$ is the critical Rayleigh number for the onset of convection[26]. However, owing to the experimental limitations in accessing the rapidly rotating, strongly supercritical regime, this scaling is not well constrained. For strong enough thermal forcing (Ra) at a given rotation rate (E), our heat transfer data conform to the non-rotating scaling behaviour. Thus, we observe two distinct convective heat transfer regimes: the rotationally controlled regime, with $Nu \propto Ra^{6/5}$, and the non-rotating regime, with $Nu \propto Ra^{2/7}$.

We define the transition between these two regimes as the point of intersection between their respective scalings, $Nu = 0.16Ra^{2/7}$ and $Nu = (Ra/Ra_c)^{6/5}$. Equating the two, we solve for transitional Rayleigh and Nusselt numbers: $Ra_t = 1.4E^{-7/4}$ and $Nu_t = 0.18E^{-1/2}$. Figure 3a shows Nu normalized by the non-rotating scaling law versus Ra normalized by the transitional Rayleigh number. When $Ra < Ra_t$ ($Nu < Nu_t$), convection is constrained by the influence of rotation and heat transfer is less efficient than its non-rotating counterpart. When $Ra > Ra_t$ ($Nu > Nu_t$), heat transfer is not significantly affected by rotation and follows the non-rotating scaling. Indeed, our empirical results agree with the boundary layer transition hypothesis, which predicts that $Nu_t \propto E^{-1/2}$.

To further test our hypothesis, we measure the thicknesses of the two boundary layers from numerical experiments carried out at $E = 10^{-4}$ and $Pr = 7$ (Fig. 3b). Following refs 17, 27, we define the Ekman boundary layer thickness, δ_E, as the vertical position of the maximum value of the root-mean-square velocity, and the thermal boundary layer thickness, δ_κ, as the vertical position of the maximum value of the temperature variance (see Supplementary Information, section 2). Figure 3b illustrates that when $\delta_\kappa \approx \delta_E$, $Ra \approx Ra_t$ and the

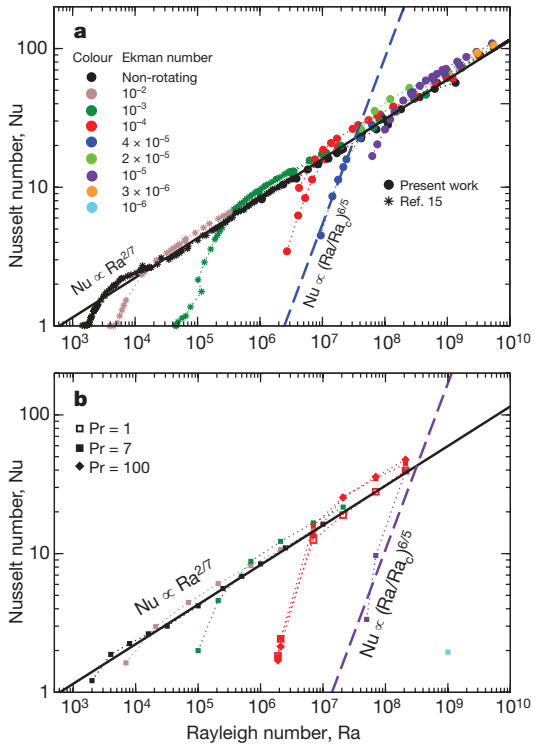

Figure 2 | Nusselt number versus Rayleigh number. **a**, Laboratory experiments; **b**, numerical simulations. Our laboratory experiments were carried out in cylinders with diameter-to-height ratios ranging from 6.25 to 1 using water ($Pr \approx 7$) and sucrose solution ($Pr \approx 10$). Included in **a** are results from ref. 15 in water. Numerical experiments are carried out in a Cartesian box with no-slip top and bottom boundaries and periodic sidewalls. Gravity and the rotation axis are both vertical. Non-rotating convection in laboratory experiments yields $Nu \propto Ra^{0.289 \pm 0.005}$ across more than five decades in Ra. Solid black lines represent the non-rotating scaling law $Nu = 0.16Ra^{2/7}$. Dashed black lines represent the rotationally controlled scaling law $Nu = (Ra/Ra_c)^{6/5}$, where $Ra_c = 6E^{-4/3}$ from ref. 26.

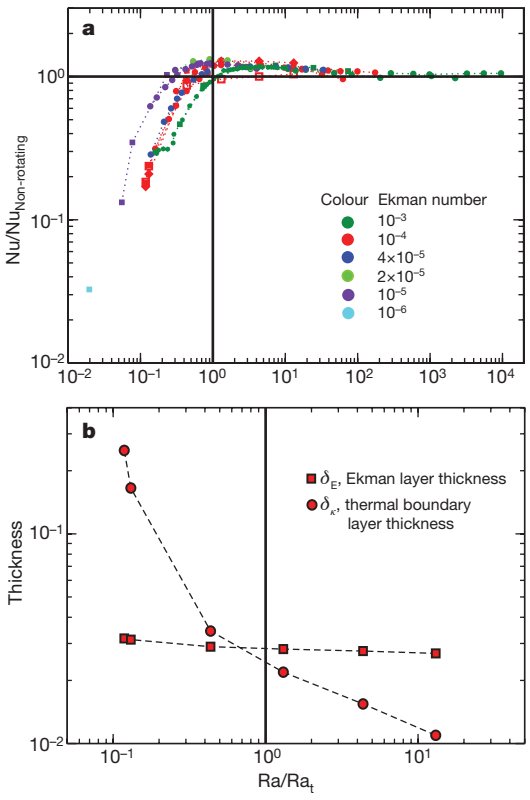

Figure 3 | The transition from rotationally controlled to non-rotating heat transfer behaviour. **a**, The heat transfer regime is determined by the transitional Rayleigh number, $Ra_t = 1.4E^{-7/4}$, for $E \leq 10^{-3}$ and $1 \leq Pr \leq 100$. Symbols are the same as in Fig. 2. The Nusselt number is normalized by its non-rotating value, $Nu_{Non\text{-}rotating} = 0.16Ra^{2/7}$. When $Ra/Ra_t > 1$, heat transfer follows the non-rotating scaling law. Near the transition, the data overshoot the non-rotating scaling law owing to Ekman pumping effects[9,30]. **b**, The numerically determined non-dimensional thicknesses of the competing boundary layers are shown as the Rayleigh number is varied for $E = 10^{-4}$ and $Pr = 7$. The dynamical transition at $Ra = Ra_t$ occurs when the relative thicknesses of the competing boundary layers are approximately equal, that is, when $\delta_\kappa = \delta_E$.

transition is in fact controlled by the relative thicknesses of the boundary layers. When the thermal boundary layer is thinner than the Ekman layer ($\delta_\kappa < \delta_E$, $Ra > Ra_t$), convection is manifested as turbulent, three-dimensional flow (Fig. 1b). Conversely, when the Ekman layer is thinner than the thermal boundary layer ($\delta_E < \delta_\kappa$, $Ra < Ra_t$), rotational effects control convection and constrain fluid motion (Fig. 1a).

It is often argued that the influence of rotation on turbulent convection dynamics is governed by the relative global magnitude of the relevant forces: the buoyancy force and the Coriolis force[7–12]. The ratio of these two global forces is represented by the convective Rossby number[7–12], $Ro_c = \sqrt{RaE^2\,Pr^{-1}}$. The force balance argument predicts a transition between rotationally controlled convection and non-rotating convection when $Ro_c \approx 1$ (see Supplementary Information, section 3), and thus predicts a transitional Rayleigh number that scales as E^{-2}, in comparison with the $E^{-7/4}$ scaling derived from our boundary layer arguments. These two scalings, when extrapolated to planetary settings, yield drastically different predictions for the importance of rotation. At a typical planetary value[12] of $E = 10^{-15}$, for example, the two scalings predict transitional Rayleigh numbers that differ by roughly four orders of magnitude. Figure 4 shows experimental heat transfer data (Nu) plotted against Ro_c. Should the force balance control the importance of rotation in convective heat transfer, we would expect the transitions to occur when $Ro_c \approx 1$. The heat transfer transitions observed in the data (Fig. 4) are not adequately explained by the global force balance, Ro_c, but are instead well described by our boundary-layer-controlled transition scaling. Furthermore, the force balance argument predicts a Pr-dependent transition, and no such dependence is observed. Our transition scaling also describes the disparate results from previous studies: those[12–14] finding the rotationally controlled $Nu \approx Ra^{6/5}$ heat transfer behaviour typically have $Ra < Ra_t$, whereas those[8–10] yielding the non-rotating scaling, $Nu \approx Ra^{2/7}$, typically have $Ra > Ra_t$, despite setting $Ro_c < 1$. To further test the validity of boundary layer control, future laboratory and numerical experiments must be able to access high Ra convection at lower values of E.

The boundary-layer-controlled transition scaling, Ra/Ra_t, is broadly applicable to natural convection systems (see Supplementary Information, section 4). The Rayleigh number, Ra, depends on a system's global density gradient (in thermal convection, the temperature gradient), which is often difficult to observe in nature. The flux-Rayleigh number, $Ra_f = RaNu$, depends instead on the overall buoyancy flux. For thermal convection, $Ra_f = \alpha_T g D^4 Q/\rho c_p \kappa^2 \nu$, where Q is the heat flux, ρ is the fluid's mean density and c_p is the fluid's specific heat. The product of Ra_t and Nu_t constitutes a transitional flux-Rayleigh number, $Ra_{f,t} = 0.25E^{-9/4}$.

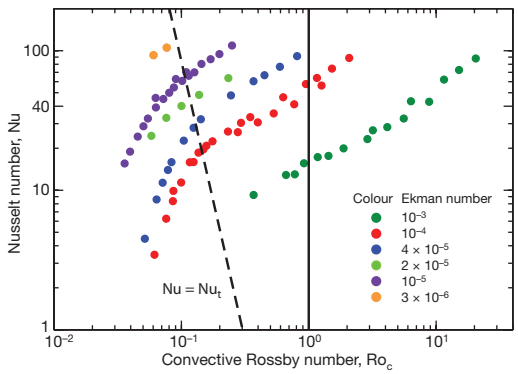

Figure 4 | Nusselt number versus the convective Rossby number for laboratory experiments in water ($Pr \approx 7$) with $3 \times 10^{-6} \leq E \leq 10^{-2}$. The convective Rossby number, Ro_c, characterizes the ratio of buoyancy forcing to the Coriolis force. Force balance arguments predict that rotation will dominate the system when $Ro_c < 1$. However, our heat transfer regime transitions follow the boundary-layer-controlled transitional Nusselt number, $Nu_t = 0.18E^{-1/2}$ (dashed line).

Thus, given the fluid properties, system size and rotation rate, as well as the emitted heat flux, a given body's convective regime can be determined. For example, a typical estimate[12,14] of the Ekman number in the Earth's liquid-metal outer core is $E \approx 10^{-15}$, which allows us to estimate a transitional flux-Rayleigh number of $Ra_{f,t} = 2 \times 10^{33}$ for the core. We estimate a flux-Rayleigh number of $Ra_f \approx 6 \times 10^{29}$ in the core using the following estimates[23,28]: $\alpha_T \approx 10^{-4}\,K^{-1}$; $g \approx 10\,m\,s^{-2}$; $D \approx 2 \times 10^6\,m$; $\rho \approx 10^4\,kg\,m^{-3}$; $c_p \approx 1{,}000\,J\,kg^{-1}\,K^{-1}$, $\kappa \approx 10^{-5}\,m^2\,s^{-1}$; $\nu \approx 10^{-6}\,m^2\,s^{-1}$; and a 4-TW superadiabatic heat flow from the core, corresponding to a superadiabatic $Q \approx 4 \times 10^{-2}\,W\,m^{-2}$. Using the empirical relation $Nu \approx (Ra/Ra_c)^{6/5}$, appropriate to convection with $Ra_f < Ra_{f,t}$, we provide the following estimate of the Rayleigh number in the Earth's core: $Ra \approx 7 \times 10^{24}$.

This estimate implies that core convection occurs just below the boundary layer transition, with $Ra/Ra_t \approx 3 \times 10^{-2}$, and this close proximity to the transition may be important for core dynamics. Recent work has shown that reversal frequencies of magnetic fields in dynamo simulations are linked to the decreasing importance of rotation[29]. Geomagnetic reversals may then depend on boundary layer dynamics and on the value of Ra/Ra_t in the core. To test the planetary and stellar applicability of our result, future work must investigate the influence of low-Pr fluids, fluid compressibility, strong magnetic fields, spherical geometry and internal heating on the boundary layer transition.

Received 27 June; accepted 28 October 2008.

1. Spiegel, E. A. Convection in stars. *Annu. Rev. Astron. Astrophys.* **9,** 323–353 (1971).
2. Ingersoll, A. P. & Porco, C. C. Solar heating and internal heat flow on Jupiter. *Icarus* **35,** 27–43 (1978).
3. Hathaway, D. H. A convective model for turbulent mixing in rotating convection zones. *Astrophys. J.* **276,** 316–324 (1984).
4. Busse, F. H. Convective flows in rapidly rotating sphere and their dynamo action. *Phys. Fluids* **14,** 1301–1314 (2002).
5. Heimpel, M., Aurnou, J. & Wicht, J. Simulation of equatorial and high-latitude jets on Jupiter in a deep convection model. *Nature* **438,** 193–196 (2005).
6. Aurnou, J., Heimpel, M., Allen, L., King, E. & Wicht, J. Convective heat transfer and the pattern of thermal emission on the gas giants. *Geophys. J. Int.* **173,** 793–801 (2008).
7. Gilman, P. A. Nonlinear dynamics of Boussinesq convection in a deep rotating spherical shell. *Geophys. Astrophys. Fluid Dyn.* **8,** 93–135 (1977).
8. Julien, K., Legg, S., McWilliams, J. & Werne, J. Hard turbulence in rotating Rayleigh-Bénard convection. *Phys. Rev. E* **53,** 5557–5560 (1996).
9. Julien, K., Legg, S., McWilliams, J. & Werne, J. Rapidly rotating turbulent Rayleigh-Bénard convection. *J. Fluid Mech.* **322,** 243–273 (1996).
10. Liu, Y. & Ecke, R. E. Heat transport in turbulent Rayleigh-Bénard convection: effects of rotation and Prandtl number. *Phys. Rev. Lett.* **79,** 2257–2260 (1997).
11. Aurnou, J. M., Heimpel, M. & Wicht, J. The effects of vigorous mixing in a convective model of zonal flow on the ice giants. *Icarus* **190,** 110–126 (2007).
12. Aurnou, J. M. Planetary core dynamics and convective heat transfer scaling. *Geophys. Astrophys. Fluid Dyn.* **101,** 327–345 (2007).
13. Christensen, U. R. Zonal flow driven by strongly supercritical convection in rotating spherical shells. *J. Fluid Mech.* **470,** 115–133 (2002).
14. Christensen, U. R. & Aubert, J. Scaling properties of convection-driven dynamos in rotating spherical shells and application to planetary magnetic fields. *Geophys. J. Int.* **166,** 97–114 (2006).
15. Rossby, H. T. A study of Bénard convection with and without rotation. *J. Fluid Mech.* **36,** 309–335 (1969).
16. Olson, P. L. & Christensen, U. R. Dipole moment scaling for convection-driven planetary dynamos. *Earth Planet. Sci. Lett.* **250,** 561–571 (2006).
17. Takeshita, T., Segawa, T., Glazier, J. A. & Sano, M. Thermal turbulence in mercury. *Phys. Rev. Lett.* **76,** 1465–1468 (1996).
18. Glazier, J. A., Segawa, T., Naert, A. & Sano, M. Evidence against ultrahard thermal turbulence at very high Rayleigh numbers. *Nature* **398,** 307–310 (1999).
19. Greenspan, H. P. *The Theory of Rotating Fluids* (Cambridge Univ. Press, 1968).
20. Hignett, P., Ibbetson, A. & Killworth, P. D. On thermal rotating convection driven by non-uniform heating from below. *J. Fluid Mech.* **109,** 161–187 (1981).
21. Boubnov, B. M. & Golitsyn, G. S. Temperature and velocity field regimes of convective motions in a rotating plane fluid layer. *J. Fluid Mech.* **219,** 215–239 (1990).
22. Read, P. L. Transition to geostrophic turbulence in the laboratory, and as a paradigm in atmospheres and oceans. *Surv. Geophys.* **22,** 265–317 (2001).
23. Tilgner, A. High-Rayleigh-number convection in spherical shells. *Phys. Rev. E* **53,** 4847–4851 (1996).
24. Verzicco, R. & Camussi, R. Prandtl number effects in convective turbulence. *J. Fluid Mech.* **383,** 55–73 (1999).

25. Schmalzl, J., Breuer, M. & Hansen, U. The influence of the Prandtl number on the style of vigorous thermal convection. *Geophys. Astrophys. Fluid Dyn.* **96,** 381–403 (2002).
26. Chandrasekhar, S. The instability of a layer of fluid heated below and subject to Coriolis forces. *Proc. R. Soc. Lond. A* **217,** 306–327 (1953).
27. Belmonte, A., Tilgner, A. & Libchaber, A. Temperature and velocity boundary layers in turbulent convection. *Phys. Rev. E* **50,** 269–279 (1994).
28. Nimmo, F., Price, G. D., Brodholt, J. & Gubbins, D. The influence of potassium on core and geodynamo evolution. *Geophys. J. Int.* **156,** 363–376 (2004).
29. Kutzner, C. & Christensen, U. R. From stable dipolar towards reversing numerical dynamos. *Phys. Earth Planet. Inter.* **131,** 29–45 (2002).
30. Kunnen, R. P. J., Clercx, H. J. H. & Geurts, B. J. Heat flux intensification by vortical flow localization in rotating convection. *Phys. Rev. E* **74,** 056306 (2006).

Supplementary Information is linked to the online version of the paper at www.nature.com/nature.

Acknowledgements Salary support for E.M.K., J.N. and J.M.A. was provided by the US National Science Foundation Earth Sciences Division Geophysics Program and the NASA Planetary Atmospheres Program. Support for S.S. and U.H. was provided by the German Research Foundation and for S.S. by the NASA Solar and Heliospheric Physics Program. Support for laboratory experiment fabrication was provided by the US National Science Foundation Instrumentation & Facilities Program. Computational resources were provided by the John von Neumann-Institut für Computing. E.M.K., J.N. and J.M.A. would like to thank J. Frydman, J. Neal, A. Yaghmaei and R. M. Aurnou for engineering support in experimental development. E.M.K. and J.M.A. would like to thank H. T. Rossby for making his thesis data available to them, J. McWilliams for discussion and S. R. Dickman for introducing them to geophysics.

Author Information Reprints and permissions information is available at www.nature.com/reprints. Correspondence and requests for materials should be addressed to E.M.K. (eric.king@ucla.edu).

doi: 10.1038/nature07647

Supplementary material for: Boundary layer control of rotating convection systems

Eric M. King[1]*, Stephan Stellmach[2,3],

Jerome Noir[1], Ulrich Hansen[2] and Jonathan M. Aurnou[1]

1 Department of Earth and Space Sciences, University of California, Los Angeles, 90095-1567 USA

*Corresponding Author, email: eric.king@ucla.edu

2 Institut für Geophysik, WWU Münster, AG Geodynamik Corrensstr. 24, Münster, 48149 Germany

3 Now at: Department of Applied Mathematics and Statistics,

and Institute of Geophysics and Planetary Physics,

University of California, Santa Cruz, 95064 USA

1 Methods

Laboratory experiments are carried out in water ($Pr \approx 7$) and sucrose solution ($Pr \approx 10$) in a 20 cm diameter right cylinder with diameter to height ratio, Γ, varying from 6.25 to 1. The tank is heated from below by a non-inductively wound electrical heating coil and rotated at up to 50 rotations per minute about a vertical axis. The temperature difference across the fluid layer, ΔT, is measured by two six-thermistor arrays imbedded in the top and bottom boundaries. The heat flux, Q, is calculated by comparing the power input to the resistor with the heating rate of coolant cycling through a thermostated bath atop the convection tank. The Biot number, Bi, characterizes the effective boundary to fluid conductance ratio: $Bi = Nu \frac{k_{fluid}}{H_{fluid}} \frac{H_{boundary}}{k_{boundary}}$, where k is thermal conductivity and H is layer thickness. For our experiments, $Bi < 0.1$, and therefore the effects of the finite conductivity in the boundaries are small[1]. The experiment is surrounded by more than 10 cm of closed-cell foam insulation to minimize sidewall heat loss.

Numerical experiments. Direct numerical simulations are carried out by solving the Boussinesq Navier-Stokes equation, energy equation, and continuity equation in a cartesian box for $Pr = 1$, $Pr = 7$, and $Pr = 100$. The box has periodic sidewalls; impenetrable, no-slip top and bottom boundaries; resolution up to $384 \times 384 \times 257$; and aspect ratio Γ varying from 1 to 4. Gravity and the rotation axis are both vertical. Fourier transform methods are employed in the horizontal directions, and Chebyshev polynomials are used in the vertical direction[2].

2 The Boundary Layer

Supplementary figure 1 shows vertical profiles of mean temperature, temperature variance, and velocity. Isothermalization of the interior fluid for $Ra/Ra_t > 1$ permits the formation of

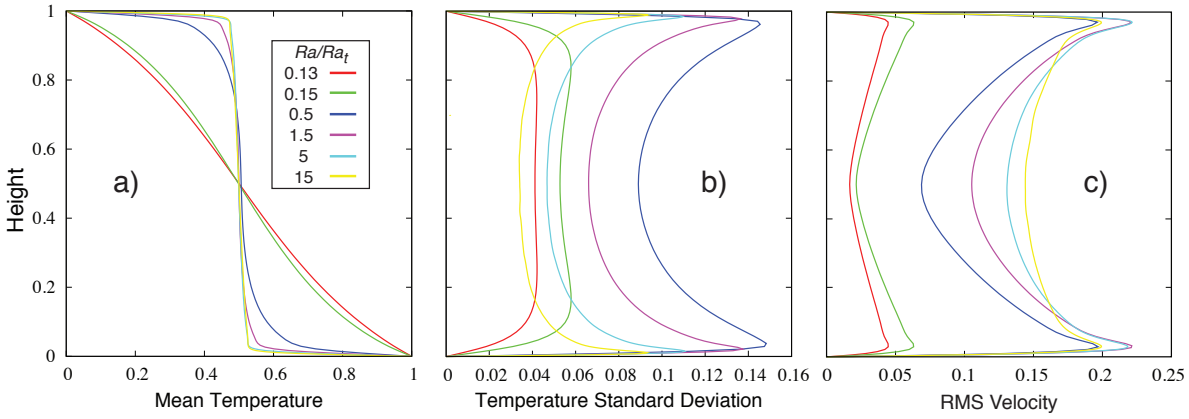

Supplementary figure 1: Vertical profiles of **a)** mean temperature (non-dimensionalized by the total temperature drop, ΔT), **b)** temperature variance, and **c)** RMS velocity (non-dimensionalized by κ/D, and normalized by $Ra^{1/2}$ for comparison) for $E = 10^{-4}$, $Pr = 7$, and $1.9 \times 10^6 \leq Ra \leq 2.1 \times 10^8$ from numerical experiments. When $Ra/Ra_t > 1$, thermal boundary layers are well-defined and the interior fluid is nearly isothermal. The thermal boundary layer thickness is well described by the height of the peak value of the temperature variance[3–6]. The height of the peak values of the RMS velocity correspond to the Ekman layer thickness[3–6].

a well defined thermal boundary layer. The thickness of this boundary layer is well described by the height of the peak value of the temperature variance[3–6], physically corresponding to the location of the development and departure of thermal plumes before they are mixed in the turbulent interior[3].

The Nusselt number, Nu, is defined as the ratio of total heat flux to overall conductive heat flux. The overall conductive heat flux is $Q_{\text{conductive}} = k\Delta T/D$, where k is the fluid's thermal conductivity, ΔT is the total temperature drop, and D is the height of the layer. In the quasi-static boundary layer, heat transfer is entirely conductive, and an isothermal interior means half the total temperature drop occurs in each (top and bottom) boundary layer. Since the total heat flux must be the same through all horizontal planes of infinite extent, the heat flux through the boundary layer equals the total heat flux,

$Q_{\mathrm{Total}} = k\Delta T/2\delta_\kappa$, where δ_κ is the thermal boundary layer thickness. The Nusselt number is then $Nu \equiv Q_{\mathrm{Total}}/Q_{\mathrm{conductive}} \approx D/2\delta_\kappa$. Supplementary figure 2 shows both Nu and $D/2\delta_\kappa$ from the $E = 10^{-4}$, $Pr = 7$ numerical experiment. The agreement between Nu and $D/2\delta_\kappa$ illustrates that the heat transfer is, in fact, well-approximated by this thermal boundary layer scaling.

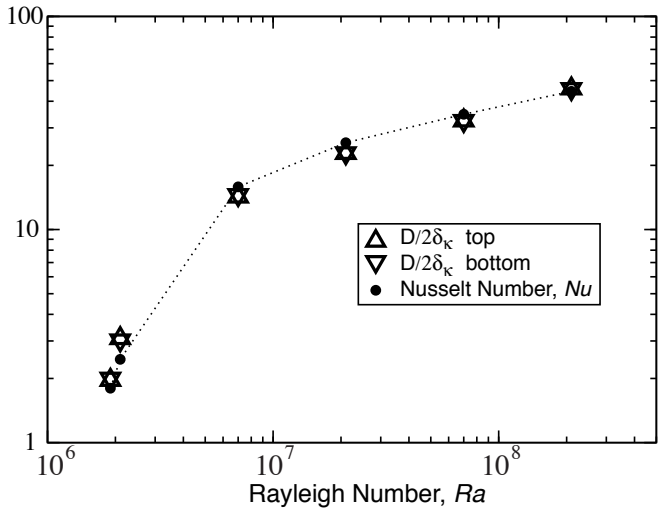

Supplementary figure 2: Nusselt number versus Rayleigh number for $E = 10^{-4}$, $Pr = 7$ numerical experiments. Also shown are thermal boundary layer data $D/2\delta_\kappa$, where δ_κ is the thermal boundary layer thickness, defined as the height of the peak value of the temperature variance[3–6]. The agreement between heat transfer measurements and boundary layer estimates shows that the boundary layer scaling of the Nusselt number, $Nu \approx D/2\delta_\kappa$, is a valid approximation.

3 Transition Scaling

The Rossby number, Ro, characterizes the strength of inertia versus Coriolis acceleration, $Ro = U/2\Omega D$, where U is a typical fluid velocity, Ω is the angular rotation rate, and D is the length scale of the system. When $Ro \ll 1$, it is thought that rotation will domi-

nate convection dynamics[7–11]. The Taylor-Proudman constraint dictates that interior flow structures will be roughly axially-invariant, and therefore quasi-two dimensional in this dynamical regime[11]. Viscosity will only become important at small ($O(E^{-1/3})$) length scales in the horizontal direction[12], and so we anticipate long, thin, axial flow structures when $Ro \ll 1$. Unfortunately, U is not directly observable in remote convection systems such as planetary interiors, and is not known a priori in experiments and simulations. The convective Rossby number, Ro_c, circumvents this difficulty by assuming inertia scales with buoyancy, thus employing the free-fall velocity assumption, $U_{\mathrm{free-fall}} \approx \sqrt{\alpha_T g \Delta T D}$, where α_T is the fluid's thermal expansion coefficient and g is gravitational acceleration. By using $U_{\mathrm{free-fall}}$, the Rossby number becomes the convective Rossby number, $Ro_c = \sqrt{\alpha_T g \Delta T / 4\Omega^2 D}$, which is the gauge typically used to predict the importance of rotation in convection systems[8–10].

According to this global force balance argument, strongly three-dimensional flow structures should not be manifested by convection with $Ro_c < 1$. We have observed, however, three-dimensional convection for $Ro_c < 1$ in our numerical experiments (Fig. 1, main text). Furthermore, heat transfer is well described by the boundary layer controlled Ra_t, and not by Ro_c (Fig. 4, main text). This indicates that Ro_c does not adequately describe the influence of rotation in convection systems.

Several other heat transfer scalings for rotating convection have been put forth. Ref. 13 develops a turbulent scaling model which predicts a transitional Rayleigh number that scales as $E^{-6/4}$. Currently, it is difficult to determine which scaling, $Ra_t \sim E^{-7/4}$ or $E^{-6/4}$, better describes the transition. In order to resolve this point, experiments must attain higher Ra with lower E. Nevertheless, in the development of the $E^{-6/4}$ transition scaling, Ref. 13 utilizes a $Nu \sim Ra^{1/3}$ non-rotating law, which is not supported by experimental studies.

Ref. 14 proposes the application of weakly non-linear theory to convective heat transfer for $Ra/Ra_t < 1$, which predicts $Nu \sim Ra/Ra_c$. However, we find the steeper, empirical

$Nu = (Ra/Ra_c)^{6/5}$ scaling better fits our data, as in many rotating convection and dynamo simulations in spherical shells[15,16].

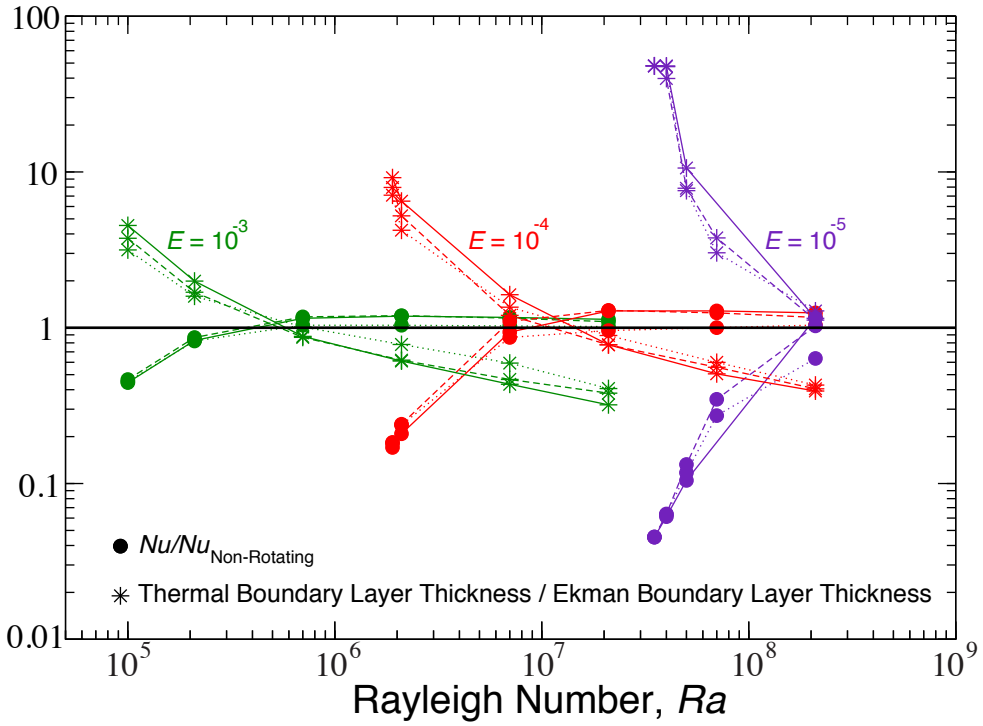

Supplementary figure 3: Boundary layer control of heat transfer transitions for $10^{-5} \leq E \leq 10^{-3}$ and $1 \leq Pr \leq 100$ from numerical experiments. Circles depict Nu normalized by the non-rotating scaling law, $Nu = 0.16Ra^{2/7}$. Stars represent the ratio of the thermal boundary layer thickness to the Ekman boundary layer thickness. The Ekman layer thickness is defined as the mean height of the peak value of the RMS velocity[3–5]. Three different Pr values are shown: $Pr = 1$, dotted lines; $Pr = 7$, dashed lines; $Pr = 100$, solid lines. The heat transfer data cross unity approximately where the boundary layer ratios cross unity. This supports our hypothesis, which predicts that heat transfer will conform to the non-rotating behavior when the thermal boundary layer becomes thinner than the Ekman boundary layer. Note also that the first order behavior of these quantities is independent of Pr, in further agreement with our boundary layer transition hypothesis.

In the main text fig. 3b, we show that the boundary layers cross when $Ra \approx Ra_t$, as predicted, for the $E = 10^{-4}$, $Pr = 7$ numerical case. To show more generally the relationship between the boundary layers and heat transfer, we must look at several different E and Pr values. In supplementary figure 3, we plot Nu, normalized by the non-rotating scaling, versus Ra for $10^{-5} \leq E \leq 10^{-3}$ and $1 \leq Pr \leq 100$ from numerical experiments. The heat transfer transition occurs where this ratio, $Nu/Nu_{\mathrm{Non-Rotating}}$, crosses unity. In the same figure, we plot the the ratio of the thermal boundary layer thickness to the Ekman boundary layer thickness. For each Ekman number, the heat transfer transition occurs where the boundary layers cross. Also notable is that the Prandtl number has no first-order effect on this behavior. These results support our hypothesis that boundary layer dynamics control heat transfer transitions across a broad range of E and Pr.

4 Free-Slip Boundary Simulations

Ref. 17 shows that the thermal wind balance, the phenomenon responsible for 'spinning up' plumes to form Taylor columns in systems with free-slip boundaries, becomes important at a distance from the boundary that scales as $E^{1/2}$. This free-slip version of the Ekman layer, called the thermal Ekman layer, is the vertical distance from the boundary over which rotation is able to respond to density perturbations and influence plume formation. Ref. 7 shows further that the boundary layer response to lateral variations of temperature is identical for no-slip and free-slip boundary conditions. Since lateral temperature variations are necessary for thermal convection to occur, the thermal Ekman layer is likely to be dynamically important in rotating convection systems with free-slip boundaries. We further hypothesize, then, that the boundary layer control arguments put forth in the main text should apply to rotating convection systems with free-slip boundaries.

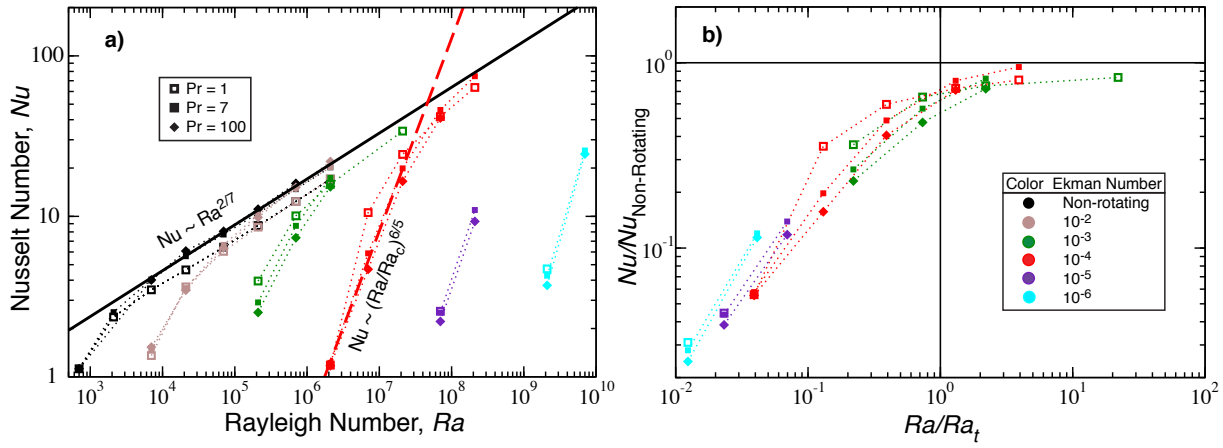

Supplementary figure 4: Heat transfer in rotating convection with free-slip boundaries, $10^{-6} \leq E \leq \infty$, and $1 \leq Pr \leq 100$. **a)** The Nusselt number as a function of the Rayleigh number. Non-rotating heat transfer follows a $Nu = 0.33Ra^{2/7}$ scaling. Rotating convection follows $Nu = (Ra/Ra_c)^{6/5}$ for $Ra/Ra_t < 1$. **b)** The Nusselt number normalized by the non-rotating scaling is shown versus Ra/Ra_t, where $Ra_t = 5.3E^{-7/4}$. When $Ra/Ra_t > 1$, rotating heat transfer conforms to the non-rotating scaling.

We have carried out a complementary suite of numerical rotating convection experiments with free-slip boundaries. Heat transfer data from the free-slip simulations are shown in supplementary figure 4a. Non-rotating heat transfer is well described by $Nu = 0.33Ra^{2/7}$. Rapidly-rotating convective heat transfer, as in the no-slip experiments, is adequately described by $Nu = (Ra/Ra_c)^{6/5}$, where Ra_c is the critical Rayleigh number for the onset of convection. We use $Ra_c = 9E^{-4/3}$ for free-slip boundaries[11]. For sufficiently large Ra, rotating convective heat transfer switches to the non-rotating scaling. We define the transitional Nusselt and Rayleigh numbers, Nu_t and Ra_t, as the point of intersection between the two scalings, yielding $Nu_t = 0.53E^{-1/2}$ and $Ra_t = 5.3E^{-7/4}$. Supplementary figure 4b shows that, as for the no-slip experiments, the transition in heat transfer behavior is well described by the transitional Rayleigh number, Ra_t.

This transition scaling agrees with the boundary layer controlled scaling derived in the

main text. That the boundary layer controlled transition pertains to free-slip convection suggests that our results can be applied to convection systems that are not contained by rigid boundaries, such as stars and gas planets.

References

[1] Verzicco, R. Effects of non-perfect thermal sources in turbulent thermal convection. *Phys. Fluids* **16**, 1965-1979 (2004).

[2] Stellmach, S., and Hansen, U. An efficient spectral method for the simulation of dynamos in Cartesian geometry and its implementation on massively parallel computers. *Geochem. Geophys. Geosyst.* **9**. Q05003 (2008).

[3] Tilgner, A., Belmonte, A., Libchaber, A. Temperature and velocity profiles of turbulent convection in water. *Phys. Rev. E* **47**, (1993).

[4] Belmonte, A., Tilgner, A., Libchaber, A. Boundary layer length scales in thermal turbulence. *Phys Rev. Lett.* **70**, 4067-4070 (1993).

[5] Belmonte, A., Tilgner, A., Libchaber, A. Temperature and velocity boundary layers in turbulent convection. *Phys. Rev. E* **50**, (1995).

[6] Takeshita, T., Segawa, T., Glazier, J. A., Sano, M. Thermal turbulence in mercury. *Phys. Rev. Lett.* **76**, 1465-1468 (1996).

[7] Julien, K., Legg, S., McWilliams, J., & Werne, J. Rapidly rotating turbulent Rayleigh-Bénard convection. *J. Fluid Mech.* **322**, 243-273 (1996).

[8] Julien, K., Legg, S., McWilliams, J., Werne, J. Hard turbulence in rotating Rayleigh-Benard convection. *Phys. Rev. E* **53**, 50306 (1996).

[9] Liu, Y. & Ecke, R. E. Heat transport in turbulent Rayleigh-Bénard convection: effects of rotation and prandtl number. *Phys. Rev. Lett.* **79**, 2257-2260 (1997).

[10] Aurnou, J. M., Heimpel, M., & Wicht, J. The effects of vigorous mixing in a convective model of zonal flow on the ice giants. *Icarus* **190**, 110-126 (2007).

[11] Chandrasekhar, S. The instability of a layer of fluid heated below and subject to Coriolis forces. *Proc. Roy. Soc. A.* **217**, 306-327 (1953).

[12] Stellmach, S., Hansen, U. Cartesian convection driven dynamos at low Ekman number. *Phys. Rev. E* **70**, 056312 (2004).

[13] Canuto, V. M., Dubivikov, M. S. Two scaling regimes for rotating Rayleigh-Benard convection. *Phys. Rev. Lett.* **80**, 281-284 (1998).

[14] Ecke, R. E. Comment on "Two scaling regimes for rotating Rayleigh-Benard convection". *Phys. Rev. Lett.* **83**, 2678 (1999).

[15] Christensen, U. R. Zonal flow driven by strongly supercritical convection in rotating spherical shells. *J. Fluid Mech.* **470**, 115-133 (2002).

[16] Christensen, U. R., & Aubert, J. Scaling properties of convection-driven dynamos in rotating spherical shells and application to planetary magnetic fields. *Geophys J. Int.* **166**, 97-114 (2006).

[17] Hide, R. The viscous boundary layer at the free surface of rotating baroclinic fluid. *Tellus* **16**, 523-529 (1964).

differentiation of other subcellular structures[9,10] in iPS-cell-derived motor neurons should help to determine why the disease is specific to motor neurons, with other types of neurons being unaffected. ■

Michael Sendtner is at the Institute of Clinical Neurobiology, University of Würzburg, Zinklesweg 10, 97078 Würzburg, Germany.
e-mail: sendtner_m@klinik.uni-wuerzburg.de

1. Ebert, A. D. *et al. Nature* **457,** 277–280 (2009).
2. Schrank, B. *et al. Proc. Natl Acad. Sci. USA* **94,** 9920–9925 (1997).
3. Wang, J. & Dreyfuss, G. *J. Biol. Chem.* **276,** 9599–9605 (2001).
4. Takahashi, K. & Yamanaka, S. *Cell* **126,** 663–676 (2006).
5. Hanna, J. *et al. Science* **318,** 1920–1923 (2007).
6. Dimos, J. T. *et al. Science* **321,** 1218–1221 (2008).
7. Lobsiger, C. S. & Cleveland, D. W. *Nature Neurosci.* **10,** 1355–1360 (2007).
8. Di Giorgio, F. P., Boulting, G. L., Bobrowicz, S. & Eggan, K. C. *Cell Stem Cell* **3,** 637–648 (2008).
9. Nishimune, H., Sanes, J. R. & Carlson, S. S. *Nature* **432,** 580–587 (2004).
10. Jablonka, S., Beck, M., Lechner, B. D., Mayer, C. & Sendtner, M. *J. Cell Biol.* **179,** 139–149 (2007).

FLUID DYNAMICS

Rotating convection on the edge

Peter L. Read

Turbulent convection in a rotating body is a common but poorly understood phenomenon in astrophysical and geophysical settings. Consideration of boundary effects offers a fresh angle on this thorny problem.

Heat energy is transported by three basic processes: conduction, radiation and convection. But which of them is likely to dominate in any given circumstance? In particular, how can we quantify the relative efficiency of each process, not least of convection, which is inherently nonlinear and turbulent? This problem is especially challenging for understanding the evolution and interior structure of stars and planets — a task that is further complicated by the fact that most stars and planets are rotating, which may modify the style of convection and influence its efficiency.

In a study that combines laboratory measurements and numerical simulations over an unusually wide range of parameters, King and colleagues (page 301 of this issue)[1] have systematically investigated the behaviour of convective heat transport in a rotating fluid. They focus on exploring the hypothesis that the type of convection that occurs is primarily governed by the ratio of the characteristic thicknesses of the principal (rotationally controlled) boundary layers (Fig. 1).

It is traditional in fluid mechanics to characterize quantities in terms of dimensionless ratios. So the total heat flux carried by a fluid can be quantified by comparing it with that obtained by conduction alone in a solid with the same thermal properties. The resulting ratio is known as the Nusselt number, Nu. This is convenient because, for many problems, the conductive heat flux is relatively easy to calculate from basic geometrical and physical properties of the fluid. Nu = 1 then corresponds to a thermal efficiency that is no better than conduction alone, whereas for convection on domestic or industrial scales, Nu takes typical values from about 10 up to several thousand.

But how should we extrapolate estimates of this convective efficiency to systems on the scale of planets or stars? From nearly 100 years of measurements and theory, several semi-empirical scaling laws have emerged that relate Nu to another dimensionless parameter, the Rayleigh number, Ra, which effectively measures the ratio of buoyancy to viscous forces in a fluid and is proportional to the imposed temperature contrast. In a non-rotating fluid, Nu has been measured[2,3] to vary as $\sim \mathrm{Ra}^{\alpha}$, where α can take a range of values ($2/7 \le \alpha \le 0.31$). The measurements cover an enormous range, including the extreme so-called 'hard' turbulence regime at values of $\mathrm{Ra} > 10^8$. This might seem to provide a good indication of how to extrapolate estimates of Nu to values of $\mathrm{Ra} \sim 10^{25}$–10^{30}, typical of planets and stars.

However, if convection takes place in a rapidly rotating fluid, things are much more complicated. This is because rapid rotation imparts an extra 'rigidity' to a fluid, but only in a direction parallel to the axis of rotation (Fig. 1). This directional rigidity changes the turbulent motions in ways that are still poorly understood, but that may profoundly influence the efficiency of convective heat transport, suggesting a scaling law closer to $\sim \mathrm{Ra}^{6/5}$ under some conditions. Such a difference in scaling exponent can change the extrapolated Nusselt number by orders of magnitude, rendering estimates of planetary or stellar heat flow extremely uncertain.

According to conventional wisdom, the force balance between buoyancy effects in the interior of the convecting region and Coriolis forces (which, for example, cause the air flow around low-pressure centres in Earth's atmosphere to circulate in the same sense as Earth's rotation) is the main factor governing the influence of rotation on the convection — notably, its efficiency as measured by Nu. King *et al.*[1] have examined whether this interior force balance provides a quantitative criterion for determining whether Nu scales either in the non-rotating limit as $\sim \mathrm{Ra}^{2/7}$ or in the rotating limit as $\sim \mathrm{Ra}^{6/5}$, but find that it doesn't predict the observed changeover between regimes.

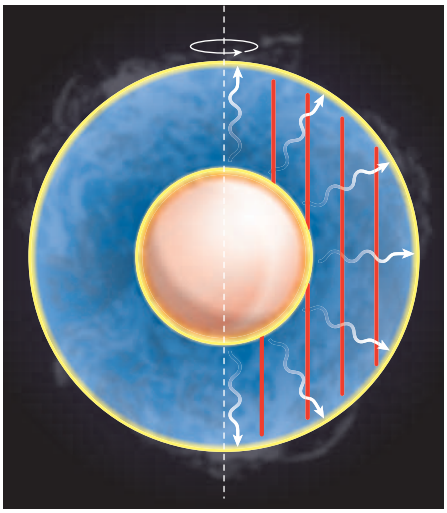

Figure 1 | Thermal convection in a spherical shell of fluid, rotating about a vertical axis. This is a situation such as might occur inside a gas-giant planet, or a stellar convection zone, and might for instance influence the planet's or star's magnetic field and other phenomena. Turbulent convective heat transfer (white arrows) is directed radially outwards, and loses heat to space. But rotation imparts a 'rigidity' parallel to the rotation axis (red bars), which may profoundly affect heat transfer. Boundary layers are shown as thick yellow lines at the inner and outer edges of the spherical shell, within which heat is added or removed and flow has to adjust to the mechanical conditions. King *et al.*[1] propose that it is the fluid dynamics at these boundary layers that constitutes the primary control on convection.

In contrast, they concentrate on the role of the boundary layers in the problem. Typical convective flows are not generally compatible with the mechanical and thermal boundary conditions imposed at the edges of the convective region. The fluid generally gets around this by creating thin regions of adjustment, known as boundary layers, in which diffusive effects (viscous or thermal) become large enough to allow the interior flow to match the imposed boundary conditions. Two types of boundary layer seem to be of most significance: first, a thermal boundary layer, dominated by thermal conduction, whose thickness $\delta_T \approx D/\mathrm{Nu}$, where D is a typical dimension of the convecting system, independent of rotation; and, second, the Ekman layer, within which viscous forces are comparable in size to Coriolis forces and whose thickness scales as $\delta_E \sim (\nu/\Omega)^{1/2}$, where Ω is the rotation rate and ν the kinematic viscosity.

King *et al.* have accumulated impressive evidence from their laboratory and numerical modelling experiments to show that the scaling dependence of Nu on Ra depends on whether $\delta_E > \delta_T$, or vice versa. This relationship seems to apply over a wide range of conditions, and even seems to work for systems bounded by stress-free boundaries, representing an idealization of

the top of the atmosphere of a planet or star.

The notion that the ratio δ_E/δ_T might determine the character and properties of rotating, stratified flows is not especially new. It was applied[4] in the 1980s to such problems as models of the circulation in the ocean thermocline, which is currently the subject of a controversy concerning Sandström's theorem on the nature and energetics of the thermohaline ocean circulation[5,6]. In that problem, the (highly turbulent) Ekman and thermal boundary layers play a clear role in the oceanic meridional circulation, so their importance in governing convective heat flow is not surprising.

In the convective problem considered by King *et al.*, however, it is less clear precisely what role the Ekman boundary layers play in the detailed transport of mass and heat. So the authors' results are all the more surprising and impressive. In the problems they have considered, however, heat enters or leaves the convecting region strictly by thermal conduction through the bounding walls, which is not exactly how heat is introduced or extracted in real planets or stars. So it remains to be seen to what extent their results can be applied to more general mechanisms for driving convection. ■

Peter L. Read is in the Subdepartment of Atmospheric, Oceanic and Planetary Physics, University of Oxford, Clarendon Laboratory, Parks Road, Oxford OX1 3PU, UK.
e-mail: p.read1@physics.ox.ac.uk

1. King, E. M., Stellmach, S., Noir, J., Hansen, U. & Aurnou, J. M. *Nature* **457,** 301–304 (2009).
2. Tilgner, A., Belmonte, A. & Libchaber, A. *Phys. Rev. E* **47,** 2253–2256 (1993).
3. Niemela, J. J., Skrbek, L., Sreenivasan, K. R. & Donnelly, R. J. *Nature* **404,** 837–840 (2000).
4. Hignett, P., Ibbetson, A. & Killworth, P. D. *J. Fluid Mech.* **109,** 161–187 (1981).
5. Wunsch, C. & Ferrari, R. *Annu. Rev. Fluid Mech.* **36,** 281–314 (2004).
6. Coman, M. A., Griffiths, R. W. & Hughes, G. O. *J. Mar. Res.* **64,** 783–796 (2006).

SYNTHETIC BIOLOGY

The yin and yang of nature

Jeff Gore and Alexander van Oudenaarden

Oscillations in gene expression regulate various cellular processes and so must be robust and tunable. Interactions between both negative and positive feedback loops seem to ensure these features.

Periodic oscillations are the basis of timekeeping. For many millennia, the main timekeeper was the water clock, in which time is recorded by the regular dripping of water into or out of a basin. In the seventeenth century, the water clock was replaced by the pendulum clock, following Galileo's famous discovery that the period of a pendulum's swing is independent of the size of the swing. This clock offered a substantial improvement because pendulum oscillations are robust and the period can be altered by changing the length of the pendulum arm. As three papers[1–3] now indicate, similar improvements are occurring in our ability to generate increasingly robust and tunable oscillations in biological systems. On page 309 of this issue, Tigges *et al.*[1] demonstrate this feat in mammalian cells, and not long ago Stricker *et al.*[2] reported it in bacteria. These two advances are nicely complemented by Tsai and colleagues' recent detailed theoretical study[3], which elucidates the essential 'design principles' underlying oscillatory networks in nature.

The simplest way to generate oscillations is by negative feedback with a delay. We are probably all familiar with this phenomenon from our attempts to maintain the proper water temperature in the shower. Because of the delay inherent in the system, we often overshoot, leading to a sometimes comical oscillation between scalding and freezing temperatures. An early example of a synthetic biological oscillator was a network called the repressilator[4], in which three genes sequentially repressed one another. The three repressive interactions led to net negative feedback, with a delay due to the multiple biochemical processes involved in gene expression. The repressilator did indeed oscillate, but the oscillations were not robust. Only half of the cells had observable oscillations, and those oscillations that did occur were variable. Moreover, the repressilator is not tunable; changing the rate constants of the various reactions generally abolishes the oscillation rather than changing its frequency[3].

Nonetheless, both robustness and tunability are important features of an oscillatory system, whether it be a gene circuit or a clock. For example, despite slight variations in the individual components of a clock, the oscillation period must remain a precise number of seconds. Similarly, if the physical environment changes, it may be necessary to retune the system to compensate: moving a pendulum clock from the ground floor to the top floor of a tall building requires retuning the clock, to correct for the small change in the acceleration due to gravity.

In the recent set of papers[1–3], a common theme is that supplementing the core negative feedback circuit with a positive feedback loop can make the oscillations both robust and tunable. Stricker *et al.*[2] demonstrated this experimentally by implementing a simple transcriptional circuit in the bacterium *Escherichia coli*. Their oscillator was composed of two genes driven by the same hybrid promoter sequence: the gene encoding the LacI protein generated the core negative feedback loop to suppress transcription, whereas that encoding the AraC protein generated the positive feedback loop. The resulting oscillation period could be tuned between 13 and 100 minutes depending on the concentration of the molecules used to induce transcription and on the temperature of the system. This oscillator design was based on a previously published theoretical study[5], although the authors[2] found it necessary to explicitly model intermediate steps such as multimerization, translation and protein folding.

Tigges *et al.*[1] construct a tunable oscillator in mammalian cells — using sense/antisense logic — by supplementing a central time-delayed negative feedback loop with a positive feedback loop. Here, negative feedback was provided by post-transcriptional repression of the gene encoding tTA by antisense RNA, whereas positive feedback was present because tTA enhanced its own transcription. The authors could tune the oscillation period by varying the number of copies of the genes encoding components of the oscillator. Whether varying the concentration of transcription inducers, while keeping the copy number of genes constant, would allow tuning of the oscillation period remains an intriguing question.

In their theoretical study, Tsai *et al.*[3] computationally analysed many different network topologies that might lead to oscillations, and also concluded that a positive feedback loop is likely to be necessary for tunable oscillations. The authors pointed out that bioengineers are simply learning tricks discovered by evolution long ago. Many biological networks that drive oscillations of variable period (such as the cell cycle) have a positive feedback loop, in addition to the central negative feedback loop that is mainly responsible for generating the oscillation. Indeed, Tsai and colleagues found that such a positive feedback loop is present in many oscillatory networks that do not require tunability (such as the circadian rhythm that tracks the day–night cycle). A possible function of the extra feedback loop in these networks of fixed frequency could be to make the oscillations robust — that is, more resistant to changes in kinetic parameters — thus perhaps increasing the 'evolvability' of the oscillation.

Advances in generating biological oscillations are similar to those made in the seventeenth century that led to our widespread adoption of the pendulum clock. What advances lie in store for our ability to construct synthetic biological oscillations? In the latest experiments[1–3], the phase of the oscillations was partly passed on to daughter cells, although individual cells gradually lost their synchronization. For any coordinated action, it is desirable for the population to oscillate in phase, thus requiring some